The Plant Cell, Vol. 11, 1277–1291, July 1999, www.plantcell.org © 1999 American Society of Plant Physiologists

Elevated Glutathione Biosynthetic Capacity in the Chloroplasts of Transgenic Tobacco Plants Paradoxically Causes Increased Oxidative Stress

Gary Creissen,[a,1] John Firmin,[a] Michael Fryer,[b] Baldeep Kular,[a] Nicola Leyland,[a] Helen Reynolds,[a] Gabriela Pastori,[a] Florence Wellburn,[c] Neil Baker,[b] Alan Wellburn,[c,2] and Philip Mullineaux[a]

[a] John Innes Centre, Norwich Research Park, Colney, Norwich NR4 7UH, United Kingdom
[b] Department of Biological and Chemical Sciences, University of Essex, Wivenhoe Park, Colchester CO4 3SQ, United Kingdom
[c] Institute of Environmental and Biological Sciences, University of Lancaster, Bailrigg, Lancaster LA1 4YQ, United Kingdom

Glutathione (GSH), a major antioxidant in most aerobic organisms, is perceived to be particularly important in plant chloroplasts because it helps to protect the photosynthetic apparatus from oxidative damage. In transgenic tobacco plants overexpressing a chloroplast-targeted γ-glutamylcysteine synthetase (γ-ECS), foliar levels of GSH were raised threefold. Paradoxically, increased GSH biosynthetic capacity in the chloroplast resulted in greatly enhanced oxidative stress, which was manifested as light intensity–dependent chlorosis or necrosis. This phenotype was associated with foliar pools of both GSH and γ-glutamylcysteine (the immediate precursor to GSH) being in a more oxidized state. Further manipulations of both the content and redox state of the foliar thiol pools were achieved using hybrid transgenic plants with enhanced glutathione synthetase or glutathione reductase activity in addition to elevated levels of γ-ECS. Given the results of these experiments, we suggest that γ-ECS–transformed plants suffered continuous oxidative damage caused by a failure of the redox-sensing process in the chloroplast.

INTRODUCTION

Plants, like all aerobic organisms, possess an array of hydrophilic and lipophilic antioxidants, such as glutathione (γ-L-glutamyl-L-cysteinyl-L-glycine [GSH]), ascorbic acid (vitamin C), phenolic isoflavanoid compounds, α-tocopherol (vitamin E), and the carotenoids, including the xanthophylls (Fryer, 1993; Mullineaux and Creissen, 1996). The reduced forms of these compounds, together with antioxidant enzymes, scavenge reactive oxygen species (ROS) and other products of oxidative reactions. These enzymes include subcellular compartment–specific isoforms of superoxide dismutase (SOD), catalase, ascorbate peroxidase (APX), glutathione *S*-transferase/glutathione peroxidase (GST/GPX), dehydroascorbate reductase, monodehydroascorbate free radical reductase, and glutathione reductase (GR). Several reduction–oxidation (redox) cycles that scavenge ROS in different subcellular compartments and that involve these enzymes and antioxidants have been proposed (e.g., the ascorbate–GSH cycle). The reducing equivalents for these reactions are derived ultimately from photosynthetic electron transport (Foyer and Halliwell, 1976; Mullineaux and Creissen, 1997). Thus, the degree of reduction of major antioxidant pools is generally considered to reflect the redox status of the tissue in question and is consequently an indicator of oxidative stress.

Glutathione, either as GSH or as GSSG (glutathione disulfide; oxidized glutathione), is regarded as a key component of antioxidant defenses in most aerobic organisms, including plants (Foyer et al., 1997). However, the high (i.e., millimolar) concentration of GSH in the chloroplast (Foyer and Halliwell, 1976; Law et al., 1983; Bielawski and Joy, 1986) is in apparent conflict with its proposed roles: the regeneration of ascorbate (Foyer and Halliwell, 1976), reduction of lipid hydroperoxides (Mullineaux et al., 1998), and regulation of chloroplast gene expression by thiol-mediated modulation of RNA polymerase subunits and protein kinases (Link, 1996).

GSH is synthesized from its constituent amino acids in an ATP-dependent two-step reaction catalyzed by the enzymes γ-glutamylcysteine (γ-EC) synthetase (γ-ECS; EC 6.3.2.2) and glutathione synthetase (GS; EC 6.3.2.3; Figure 1A). In plants, GSH biosynthesis occurs in the cytosol and the chloroplast, with at least one control point being the regulation of activity of γ-ECS (Hell and Bergmann, 1990; Ruegsegger and Brunold, 1993; Noctor et al., 1996, 1997).

[1] To whom correspondence should be addressed. E-mail creissen@bbsrc.ac.uk; fax 44-1603-456844.
[2] It is with deep regret that we report that Alan Wellburn died on May 8, 1999.

Additional regulation of GSH biosynthesis may be achieved by the supply of its constituent amino acids (Strohm et al., 1995; Noctor et al., 1997). Foliar GSH levels have been successfully raised by three- to fourfold in poplar transformed with the coding sequence of the γ-ECS gene (*gshI*) from *Escherichia coli* under the control of the cauliflower mosaic virus (CaMV) 35S promoter and overexpressing γ-ECS activity by at least 24-fold (Noctor et al., 1996). Conversely, poplar transformants overexpressing a transgene encoding *E. coli* GS did not show any increase in foliar GSH content (Strohm et al., 1995). In both sets of transgenic poplar, the products of the transgene were restricted to the cytosol.

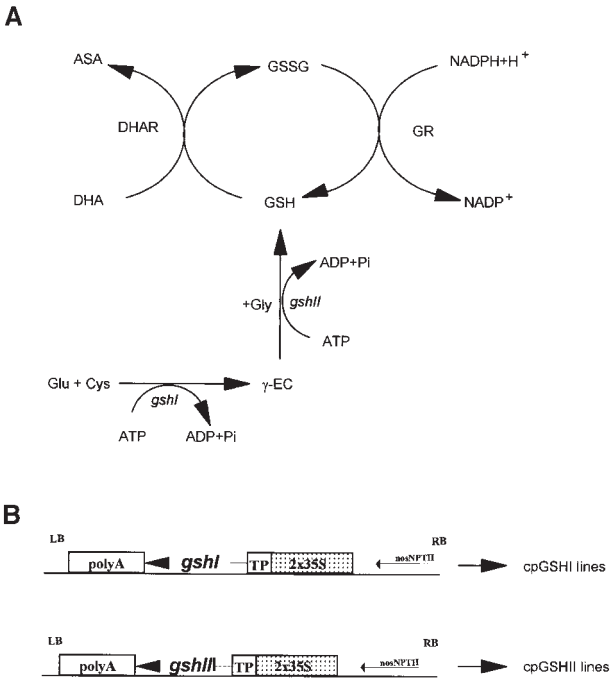

Figure 1. Synthesis and Cycling of GSH.

(A) Biosynthesis and cycling of GSH in higher plant chloroplasts (Foyer et al., 1997; Mullineaux and Creissen, 1997). ASA, ascorbic acid; DHA, dehydroascorbate; DHAR, dehydroascorbate reductase; γ-EC, γ-glutamylcysteine; GR, glutathione reductase; GSH, reduced glutathione; GSHI, γ-glutamylcysteine synthetase; GSHII, glutathione synthetase; GSSG, oxidized glutathione.

(B) Schematic diagrams of the T-DNAs of pGSH106 and pGSH209 harboring chimeric genes encoding *E. coli gshI* and *gshII*, respectively. TP is the sequence encoding the chloroplast transit peptide from the pea ribulose biphosphate carboxylase small subunit gene; 2x35S is the CaMV 35S promoter with doubled enhancer region; and polyA (for poly[A]) is the CaMV 19S polyadenylation sequence (Guerineau et al., 1988; see Methods). The chimeric genes were inserted into the T-DNA of pBIN19 (Bevan, 1984), and nosNPTII is the kanamycin resistance gene used to select tobacco transformants. LB and RB refer to the left and right borders of the pBIN19 T-DNA, respectively. Transformants were designated as cpGSHI or cpGSHII lines.

The cellular levels of ROS must be tightly regulated in plants, as they are in mammalian cells (Meyer et al., 1993). At least part of this regulation is achieved by transcriptional control: mRNAs of several components of the ROS scavenging system are induced in response to many biotic and abiotic stresses (Criqui et al., 1992; Conklin and Last, 1995; Grantz et al., 1995; Willekens et al., 1995; Karpinski et al., 1997). ROS in plants, particularly H_2O_2 and $O_2^{\cdot-}$, are also implicated in programmed cell death as part of developmental processes and in the hypersensitive response to pathogens. This response is accompanied by local and systemic changes in the redox state of the foliar GSH pool and the induction of pathogenesis-associated genes, some of which encode antioxidant enzymes (Greenberg et al., 1994; Levine et al., 1994; Baker and Orlandi, 1995; Jabs et al., 1996; May et al., 1996; Mittler et al., 1996; Pennell and Lamb, 1997; Allen and Fluhr, 1997).

Treatments of protoplasts, suspension cultures, or leaves of several different plant species with GSH induce marked changes in expression of genes encoding components of the ROS scavenging system (Hérouart et al., 1993; Wingsle and Karpinski, 1996; Karpinski et al., 1997). However, the effect of GSH is not uniform in different experimental systems. For example, treatment of bean suspension cultures with GSH strongly induces transcripts encoding chalcone synthase (CHS) and phenylalanine ammonia-lyase (PAL; Wingate et al., 1989), whereas pretreatment of Arabidopsis leaves with GSH before exposure to photoinhibitory light intensities results in a failure to induce APX transcripts that normally increase greatly in response to this stress (Karpinski et al., 1997).

Taken collectively, these data provide circumstantial evidence that in plants, the regulation of nuclear gene expression is influenced by ROS and the redox states of antioxidant pools, although to our knowledge, no regulatory factor has been isolated from plants that is specifically redox modulated. Furthermore, considerations concerning ROS homeostasis in cells are complicated by the membrane-permeable nature of some ROS, such as H_2O_2. For example, this means that increased oxidative stress in the chloroplast could have a regulatory impact on the maintenance of ROS levels in other subcellular compartments (Asada, 1994; Karpinski et al., 1997).

In this study, we report the outcome of a set of experiments with transgenic tobacco plants in which the transgene-expressed *E. coli* γ-ECS and GS were fused to the chloroplast transit peptide sequence from the small subunit of ribulose-1,5-bisphosphate carboxylase/oxygenase from pea, which ensures efficient targeting to the chloroplast stroma (Anderson and Smith, 1986; Guerineau et al., 1988; Creissen et al., 1995). In these experiments, our goals were to raise the level of GSH in chloroplasts and to determine whether doing so raised the tolerance of the plants to photooxidative stress and decreased their susceptibility to photoinhibition, thus providing a direct link among plastid redox status, ROS content, and the efficiency of photosynthesis

under adverse conditions. Paradoxically, however, increased GSH biosynthetic capacity in the chloroplast resulted in greatly enhanced sensitivity to oxidative stress. Our data indicate that a cycle of oxidative damage is established that is caused by the effects of ROS accumulation on photosynthesis. This cycle is possibly initiated by a failure of the chloroplast homeostatic mechanism that balances ROS scavenging with ROS production during photosynthesis.

RESULTS

Phenotypes of Primary (T_1) Transgenic Tobacco Plants Expressing Chloroplast-Targeted GSHI or GSHII

Plants overexpressing chloroplast GSHI (cpGSHI) and cpGSHII (Figure 1B) were recovered as kanamycin-resistant plantlets from tissue culture after leaf disc transformation with pGSH106 and pGSH209, respectively, and placed under greenhouse conditions (see Methods). Immunodetection of GSHI and GSHII in purified chloroplast fractions from transformed plants confirmed that the *E. coli* GSHI and GSHII proteins were targeted to the chloroplast (Figures 2A and 2B). Whereas cpGSHII lines were phenotypically indistinguishable from wild-type tobacco, the five independent cpGSHI lines that were recovered developed severe necrotic lesions on their leaves, a mild example of which is shown in Figure 3A (cpGSHI-24). In all cases, the necrosis developed rapidly as the leaf aged (Figure 3A); by the time the leaf in a wild-type plant would have been fully expanded, the necrotic patches on the cpGSHI-overexpressing leaves had fused and the leaves had withered. All of the cpGSHI lines were sterile under greenhouse conditions. At an earlier stage in their growth, leaf discs were cut from young prenecrotic leaves of all the cpGSHI lines and placed back in tissue culture to recover clonal propagants. These clonally propagated plants, once rooted, were placed in a controlled-environment room (see Methods). Under these conditions, the cpGSHI lines were less severely affected than were those grown under greenhouse conditions (Figure 3B). Nevertheless, as the leaves developed, they displayed spreading chlorosis, which eventually covered the leaf. Necrotic patches subsequently appeared. However, under the controlled-environment conditions, all of the lines were fertile, and thus, most subsequent work described here was performed with controlled-environment-grown plants.

Leaves of controlled-environment-grown cpGSHI lines had up to twofold higher levels of foliar H_2O_2 when compared with control material (Table 1), which confirmed that these plants were subjected to increased oxidative stress. In the greenhouse in July 1995, when the first transfer of T_1 cpGSHI lines from tissue culture occurred, the light intensity (photosynthetically active photon flux density [PPFD]) fluctuated between 700 and 900 μmol m^{-2} sec^{-1}, whereas in the controlled environment, the PPFD was a constant 250 μmol m^{-2} sec^{-1} (1 m from the lights). Therefore, we hypothesized that the cpGSHI lines were sensitive to high light intensities and that this sensitivity was manifested as oxidative damage to their chloroplasts, which induced extreme necrosis in the greenhouse and less severe chlorosis in the controlled environment.

Expression of cpGSHI and Measurement of Foliar GSH Levels

All five controlled-environment-grown cpGSHI lines had readily detectable levels of cpGSHI transcripts, immunodetectable levels of *E. coli* γ-ECS protein in their chloroplasts (data not shown), and up to 85-fold increased levels of γ-ECS activity (Table 1). GSH and γ-EC levels in leaves were elevated by up to five- and 25-fold, respectively (Table 1). Foliar cysteine levels were unchanged

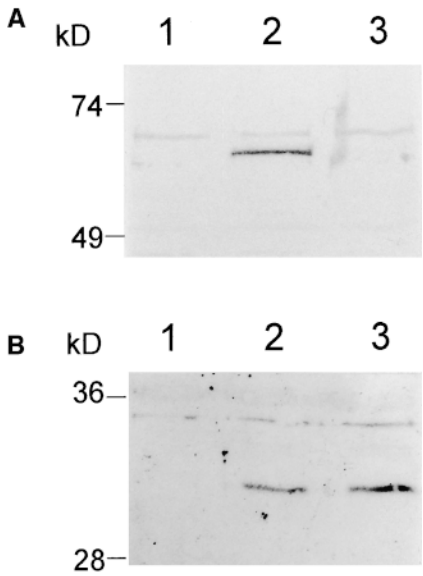

Figure 2. Localization of Transgene-Encoded γ-ECS and GS in the Chloroplast.

(A) Immunodetection of γ-ECS in purified chloroplast fractions from progeny of cpGSHI-24 × cpGSHII-1.

(B) Immunodetection of GS in purified chloroplast fractions from progeny of cpGSHI-24 × cpGSHII-1.

Chloroplast fractions (20 μg of protein per lane) free of any detectable cytosol contamination were resolved by SDS-PAGE, and γ-ECS and GS were detected on gel blots by using antisera raised against recombinant *E. coli* GSHI and GSHII (Arisi et al., 1997). Lane 1, wild type; lane 2, cpGSHI-24 × cpGSHII-1; and lane 3, cpGSHII-1. Numbers at left indicate apparent molecular weight in kilodaltons.

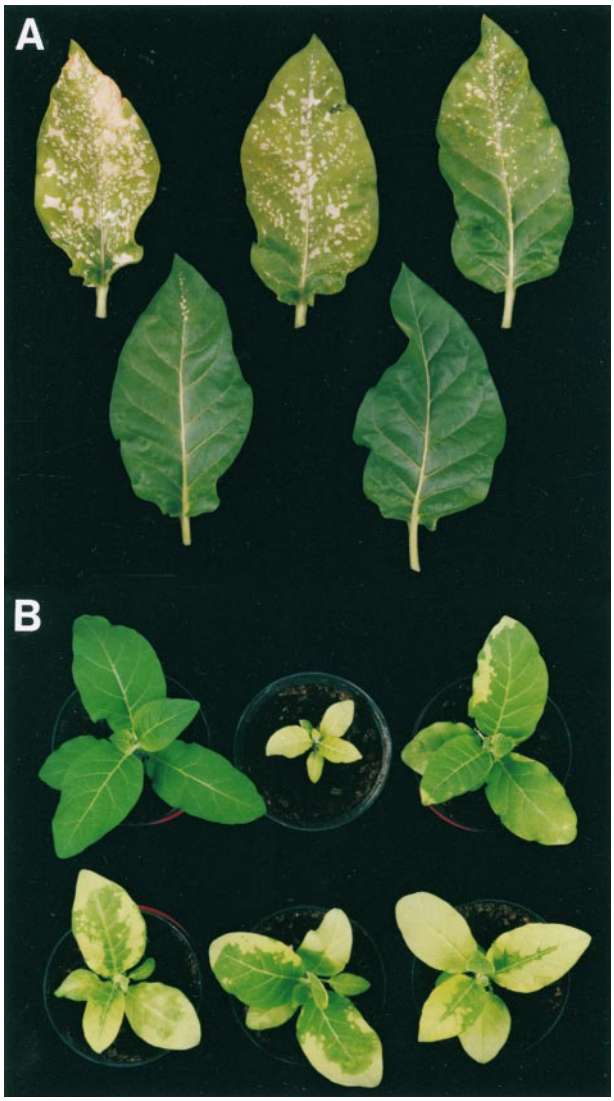

Figure 3. Phenotypes of Primary cpGSHI Transformants.

(A) Necrotic lesions on leaves from the primary transgenic line cpGSHI-24 grown under greenhouse conditions (700 to 900 μmol m^{-2} sec^{-1}). The leaves are from successive nodes (oldest at top left and youngest at bottom right).

(B) A tissue culture–derived wild-type regenerant and primary transgenic tobacco lines cpGSHI-8, cpGSHI-22, cpGSHI-26, cpGSHI-24, and cpGSHI-23 (clockwise from top left), grown under controlled-environment conditions (see Methods). The plants were regenerated from leaf explants from greenhouse-grown primary transformants, rerooted, and placed in the controlled-environment room for 3 weeks (see Results).

compared with control plants (data not shown). Transgenic plants expressing cpGSHII showed no changes in foliar GSH or γ-EC levels when compared with wild-type controls (data not shown).

The oxidative damage in the cpGSHI lines was associated with an increased capacity to synthesize GSH and was the opposite of what was anticipated (see Introduction). We hypothesized further that the greatly increased foliar levels of γ-EC, a molecule that normally does not accumulate to any degree in unstressed plant tissue (Noctor et al., 1996; Polle, 1996), may have been the cause of this phenotype.

Generation of cpGSHI × cpGSHII Hybrid Transgenic Tobacco Lines

We reasoned that the high levels of γ-EC in leaves of cpGSHI transgenic lines could perhaps be lowered and that GSH levels could be increased concomitantly by crossing these lines with a tobacco line overexpressing GS in the chloroplast (cpGSHII-1). Such crosses were performed with cpGSHI-8 and cpGSHI-24, two cpGSHI lines that represented extremes in the severity of the symptoms (see Figure 3B). Progeny were screened using protein gel blotting (see Methods) for those individuals containing cpGSHI, cpGSHII-1, both transgenes (cpGSHI × cpGSHII-1 hybrids, hereafter termed cpGSHI/II hybrids), or no transgene (the wild type). Both crosses produced cpGSHI/II hybrid progeny that showed a distinct amelioration of symptoms compared with their cpGSHI siblings, although a wild-type phenotype was not achieved in the cpGSHI/II hybrid groups (Figures 4A and 4B).

GSH Determinations in the cpGSHI/II F_2 Hybrid Progeny

The cpGSHI/II hybrid progeny from crosses with the two different cpGSHI lines had up to sixfold elevated levels of foliar glutathione (GSH and GSSG) than their wild-type recessive siblings and up to threefold higher levels than those siblings expressing only the extra chloroplast γ-ECS (cpGSHI alone; Figure 5). Similarly, the levels of total γ-EC (γ-EC plus di-γ-glutamylcystine [ESSE]) were higher than those in cpGSHI siblings. However, there was also a marked increase in the redox states of these two thiol pools in both sets of cpGSHI/II hybrids compared with their cpGSHI siblings. Thus, the hybrids contained more GSH and γ-EC and less GSSG and ESSE than did their cpGSHI siblings (Figure 5). Therefore, amelioration of the oxidative stress symptoms in cpGSHI/II hybrids compared with their cpGSHI counterparts was associated with changes in the redox status of the GSH and γ-EC pools in favor of their reduced forms. Cysteine pools were not affected by any combination of transgenes in progeny arising from these crosses (data not shown).

Table 1. GSH, γ-EC, and H_2O_2 Levels and γ-ECS Activity in Leaves of Primary cpGSH Transgenic Lines[a]

Parameter	WT[b]	cpGSHI-8	cpGSHI-22	cpGSHI-23	cpGSHI-24	cpGSHI-26
GSH[c]	298 ± 54	1270 ± 168	889 ± 117	1169 ± 177	1675 ± 176	1546 ± 156
γ-EC[c]	6.2 ± 1.4	81 ± 14.5	35.8 ± 4.1	160 ± 14.2	103.7 ± 11.9	81 ± 14.5
H_2O_2[c]	463 ± 87	976 ± 115	880 ± 80	1128 ± 80	929 ± 120	837 ± 117
γ-ECS activity[d]	25	2140	2156	1042	219	471

[a] Samples were collected from leaves (node 4) of controlled-environment-grown plants ~4 weeks after transfer from in vitro culture. GSH and γ-EC were determined as described in the legend of Figure 5. H_2O_2 was determined fluorometrically according to Guilbault et al. (1967; see Methods), and γ-ECS activity was determined in crude cell-free extracts as the rate of formation of γ-EC from cysteine under anaerobic conditions (see Methods).

[b] WT,wild type.

[c] Given as nanomoles per gram fresh weight of tissue.

[d] Given as nanomoles per gram fresh weight of tissue per minute.

Generation of Hybrids between GR Transformants and cpGSHI Plants

To determine whether it was the change in the redox state of both or only one of the thiol pools in cpGSHI/II hybrids compared with their cpGSHI siblings that was responsible for the amelioration of the chlorotic symptoms, we crossed, as a pollen donor, a transgenic tobacco plant harboring up to 10-fold higher levels of GR in its chloroplasts (tobacco line GR46-27; Creissen et al., 1995) with homozygous cpGSHI-8 and cpGSHI-24. In GR46-27 × cpGSHI progeny from the two crosses, there was no amelioration of chlorotic symptoms, although there was an elevation of the redox state of the GSH pool by a minimum of 40% compared with cpGSHI controls (Table 2). In vitro, GR was only inhibited <10% by γ-EC or ESSE at concentrations 10-fold in excess of those encountered in the cpGSHI leaves; also, GR was not able to use ESSE as a substrate (data not shown). Furthermore, extractable GR activity from leaves of cpGSHI lines was at least equivalent to that from their wild-type siblings (data not shown). Therefore, GR was unlikely to be inhibited in vivo by the enhanced levels of γ-EC or ESSE.

Photosynthesis and Chloroplast Integrity

The sensitivity of the cpGSHI-containing transgenic lines to light intensity was confirmed when the performance of photosynthesis (measured as light-dependent CO_2 fixation) was measured as a function of PPFD (Figure 6). For plants grown in controlled-environment conditions, the saturation of CO_2 fixation occurred at ~800 μmol m^{-2} sec^{-1} for both wild-type (transgene recessive) and cpGSHII-1 progeny (Figure 6). These light saturation curves are typical of plants grown under low-light conditions (Baker, 1994). cpGSHI progeny showed a much-depressed capacity for photosynthesis as revealed by the saturation of CO_2 fixation at a PPFD of ~250 μmol m^{-2} sec^{-1}, and saturation of CO_2 fixation in the cpGSHI/II hybrids occurred at ~500 μmol m^{-2} sec^{-1} (Figure 6). Without exception, progeny from the cpGSHI-8 × cpGSHII-1 cross showed an identical pattern of response in these experiments to that of the cpGSHI-24 × cpGSHII-1 hybrid group shown in Figure 6. It is important to note that the leaf disc samples for the photosynthesis experiments were taken from just fully expanded leaf sections that did not display any chlorosis. Thus, the poor photosynthetic performance of the cpGSHI lines was not an immediate consequence of loss of chlorophyll, although subsequent measurements of photosynthetic parameters in chlorotic tissues displayed a yet further worsening of chloroplast function (data not shown).

Ultrastructural analysis of chloroplasts in green sectors of cpGSHI lines (Figures 7A and 7B show cpGSHI-8) revealed the presence of spherical bodies sandwiched between the stroma thylakoids of otherwise normal-looking chloroplasts (cf. Figures 7A and 7C). The nature of the spherical bodies has not been investigated further. Similar images in chlorotic and necrotic tissues revealed swelling and then deterioration in chloroplast grana, and under these conditions the spherical bodies were no longer evident (Figure 7B).

Expression of Genes Encoding Components of the ROS Scavenging System and Pathogenesis-Associated Genes in the cpGSHI Lines

The oxidative stress phenotype and elevated foliar H_2O_2 levels suggest that the foliar transcript levels of several stress-responsive genes encoding proteins important in pathogen responses and parts of the plant's antioxidant defenses should be elevated (see Discussion). Therefore, the cpGSHI lines grown in controlled-environment conditions were

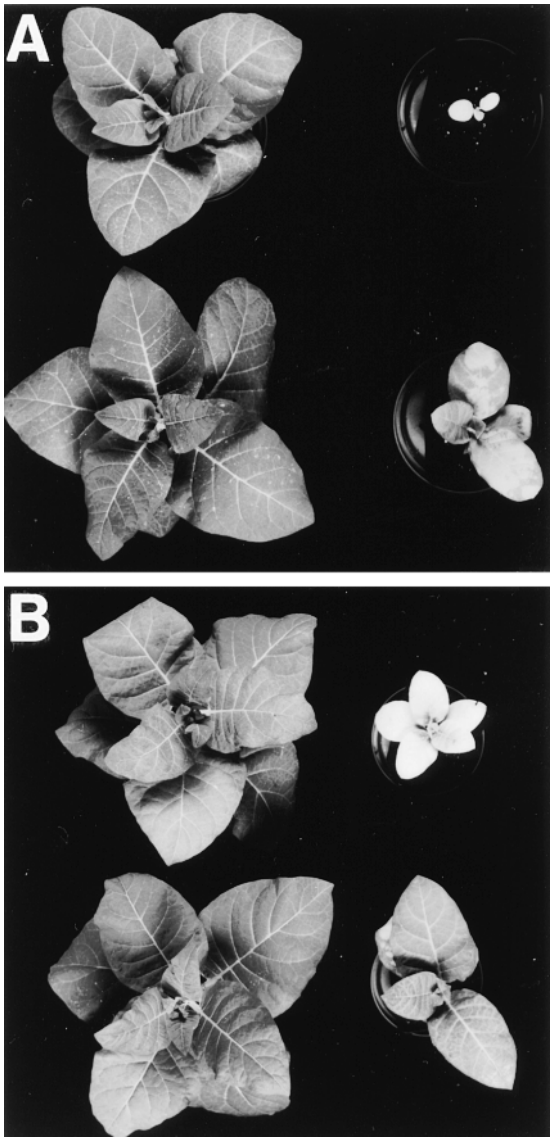

Figure 4. Progeny Resulting from cpGSHI-8 × cpGSHII-1 and cpGSHI-24 × cpGSHII-1 Crosses.

(A) cpGSHI-8 × cpGSHII-1.
(B) cpGSHI-24 × cpGSHII-1.
All plants were 4 weeks old and were grown under controlled-environment conditions. Genotypes clockwise from bottom left in **(A)** and **(B)** are double transgene recessive (wild type), cpGSHII-1, cpGSHI, and cpGSHI/cpGSHII-1 hybrid. The genotypes of individual progeny from these crosses were identified by immunoblot screening by using antisera specific to the *E. coli* γ-ECS (in cpGSHI-lines) and GS (in cpGSHII-1) (see Methods; Arisi et al., 1997).

screened for the levels of the transcripts that encode Fe–SOD, Mn–SOD, Cu/Zn SOD (plastidial and cytosolic isoforms), GR (plastidial and cytosolic isoforms), peroxisomal catalase, phospholipidhydroperoxide (PH)–GPX, GST/GPX, APX (cytosolic isoform), monodehydroascorbate free radical reductase, CHS, PAL, and pathogenesis-related protein 1 (PR-1a). Surprisingly, the levels of none of these transcripts were elevated (data not shown). However, in four independent experiments in which plants were dark adapted for 72 hr and subsequently exposed to the controlled-environment light levels, Fe–SOD transcript accumulation was slower in cpGSHI-24 than in the wild type (Figure 8). In a more limited experiment with greenhouse-grown material displaying severe necrotic symptoms, the PR-1a transcript was substantially induced (Figure 9).

Effects on Catalase Expression

Tobacco plants that have much reduced peroxisomal catalase activity display a light intensity–dependent necrosis and induction of PR-1a very similar to the symptoms described here for the plants overexpressing γ-ECS in their chloroplasts (see Discussion; Willekens et al., 1997). Therefore, we investigated whether the phenotype in the cpGSHI-transformed plants could have been caused by an impairment of catalase activity. Foliar catalase activity was approximately twofold higher in the cpGSHI lines compared with their recessive siblings (Table 3). Therefore, the light intensity–dependent oxidative stress described here was not caused by an inhibition of catalase activity, in keeping with the lack of perturbation of catalase mRNA levels (data not shown).

DISCUSSION

The photosynthetic apparatus is particularly susceptible to oxidative damage, despite an apparently well-developed plastidial ROS scavenging system (see Introduction). Therefore, we reasoned that any increased capacity of the chloroplast to synthesize a key antioxidant such as GSH would make leaves and, therefore, the plant less susceptible to oxidative stress. From the data presented in this study, clearly an increase in total foliar GSH and γ-EC can be achieved by targeting to the chloroplast extra γ-ECS activity alone (in cpGSHI lines) and even more by enhancing this activity with that of GS (in cpGSHI/II hybrid lines; Table 1 and Figure 5). Paradoxically, enhanced capacity for GSH biosynthesis in these transgenic plants was associated with a light-dependent chlorotic/necrotic phenotype (Figures 3 and 4). The characteristics of these transgenic plants and considerations of how such properties came about are summarized in the following sections.

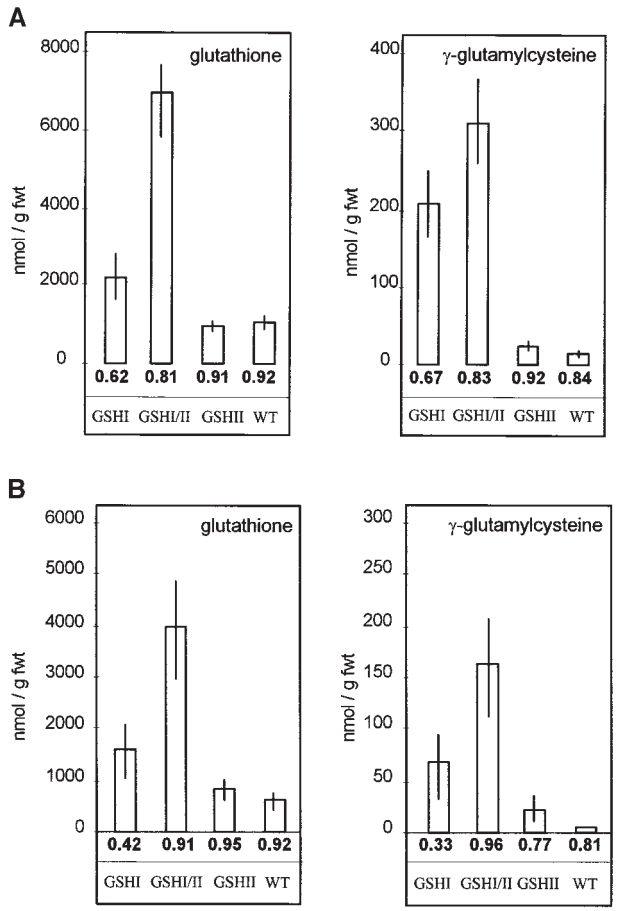

Figure 5. Foliar GSH (GSH plus GSSG) and γ-EC (γ-EC plus ESSE) in cpGSHI × cpGSHII-1 Hybrids.

(A) Total GSH and γ-EC in progeny of cpGSHI-8 × cpGSHII-1.
(B) Total GSH and γ-EC in progeny of cpGSHI-24 × cpGSHII-1.
Values are in nanomoles per gram fresh weight (fwt) for GSH plus GSSG (left) and for γ-EC plus ESSE (right). The redox states of these compounds (GSH/[GSH + GSSG]; γ-EC/[γ-EC + ESSE]) and the genotype of the progeny are shown beneath the histograms. The histograms are the means from at least three leaf samples from four individual plants (a minimum of $n = 12$) of each progeny genotype, and the vertical lines are the standard error of their means. GSH and γ-EC were determined from neutralized acid extracts by derivitization with monobromobimane (Newton et al., 1981), separation of the products by reversed-phase HPLC, and quantification using an online fluorometer. Aliquots of the neutralized extracts were treated with DTT to reduce oxidized thiols and then treated as described. For more details, see Methods. WT, wild type.

The Chlorotic/Necrotic Phenotypes Are a Consequence of Oxidative Stress

The most severe chlorotic/necrotic phenotypes were observed in those lines expressing only γ-ECS (i.e., cpGSHI lines), and the severity of the phenotype was ameliorated when extra GS activity was present in the cpGSHI/II hybrids (Figures 3 and 4). The cpGSHI lines possessed enhanced foliar thiol pools (i.e., both GSH and γ-EC), which were primarily in the oxidized state (Figure 5); therefore, the severity of the symptoms was associated with the low redox state of the GSH and γ-EC pools.

Because the cpGSHI/II hybrids had more foliar GSH (GSH plus GSSG) and because this pool was in a more reduced state compared with their cpGSHI siblings (Figure 5), the possibility that the high levels of GSH were the cause of the chlorosis could be eliminated. This ruled out the inhibition of thiol-sensitive antioxidant enzymes such as plastidial APX and violaxanthin de-epoxidase (Asada, 1994; Foyer and Harbinson, 1994) as causes of the observed phenotype.

Foliar H_2O_2 levels in the cpGSHI lines were approximately double those in the wild-type material (Table 1). Furthermore, H_2O_2 levels in the cpGSHI/II hybrid progeny were intermediate between those of their wild-type and cpGSHI siblings (data not shown). The considerations listed above and these data indicate that these plants were suffering increased levels of oxidative stress. This could be brought about by either an increase in ROS production or a defect in ROS scavenging. These possibilities are not mutually exclusive.

Possible Cause of the Lowered Redox State of the GSH Pool in cpGSHI Transformants

The cpGSHI/II hybrid leaves contained up to twice the level of total GSH as did their cpGSHI siblings and yet this GSH was in a more reduced state (Figure 5). Thus, the low redox state of the GSH pool in cpGSHI plants cannot be due

Table 2. Redox State of the Foliar Glutathione Pool in cpGSHI-8 × GR46-27 and cpGSHI-24 and GR46-27 Progeny

Genotype[a]	GSH/(GSH + GSSG)[b]
cpGSHI-8	0.36
cpGSHI-8 × GR46-27	0.51
cpGSHI-24	0.19
cpGSHI-24 × GR46-27	0.39
GR46-27	>0.95
Wild type	>0.95

[a] cpGSHI/GR46-27 hybrid progeny were confirmed using the anti–γ-ECS antiserum and detection of cotransferred luciferase activity (Creissen et al., 1995), respectively. Control material was homozygous progeny of GR46-27 (Creissen et al., 1995), cpGSHI lines, and wild-type tobacco cultivar Samsun.

[b] GSH and GSSG were detected in the same sample by amperometric detection after separation by HPLC (see Methods). The redox state of the glutathione pool in each of the genotypes was determined from three individual plants and three leaf samples from each plant ($n = 9$).

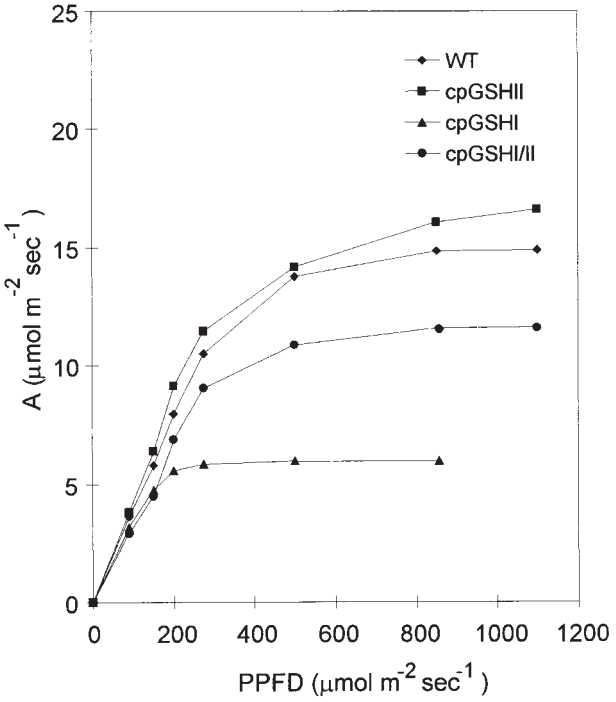

Figure 6. CO_2 Assimilation in Response to Changes in Incident PPFD.

Response of CO_2 assimilation (A), corrected for dark respiration, to PPFD was measured in the third leaves of wild-type, cpGSHI, cpGSHII, and cpGSHI/II plants. Data points are the means of five replicates, and standard errors were below 10% of these means in all cases.
WT, wild type.

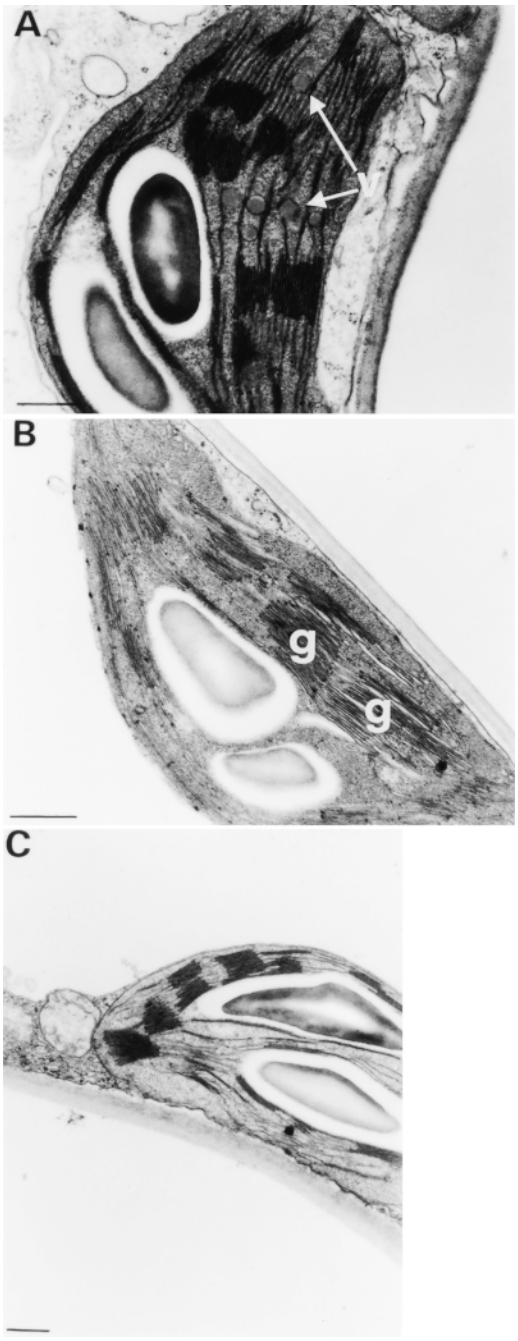

Figure 7. Transmission Electron Microscopy of Chloroplasts from Leaf Tissue of cpGSHI-8 and Wild-Type Tobacco.

(A) Chloroplast from a cpGSHI-8 green leaf showing presence of spherical vesicles (v) in the stroma between stromal thylakoids.
(B) Chloroplast from chlorotic tissue of cpGSHI-8 showing swollen granum thylakoids (g).
(C) Chloroplast from healthy leaf tissue of tobacco cultivar Samsun. Bars = 0.5 μm.

entirely to an inability to reduce any GSSG that is formed during normal cellular oxygen metabolism. We could find no evidence that GR activity was inhibited in the cpGSHI lines or that γ-EC or ESSE could be a substrate for or act as an inhibitor of the enzyme in vitro (see Results). The oxidative stress phenotype was not ameliorated in cpGSHI × GR46 hybrid progeny that contained up to 10-fold elevated levels of plastidial GR activity from a CaMV 35S–pea GR transgene (see Results; Broadbent et al., 1995; Creissen et al., 1995). This was despite a minimum of a 40% increase in the redox state of the GSH pool in these hybrids compared with cpGSHI controls (Table 2). We conclude that the lowered redox state of the GSH pool was not the direct initiator per se of the chlorotic/necrotic phenotype in the cpGSHI lines.

Possible Causes for the Accumulation of ESSE

γ-EC and ESSE also accumulated in the leaves of cpGSHI lines and in their cpGSHI/II siblings. Wild-type plants under

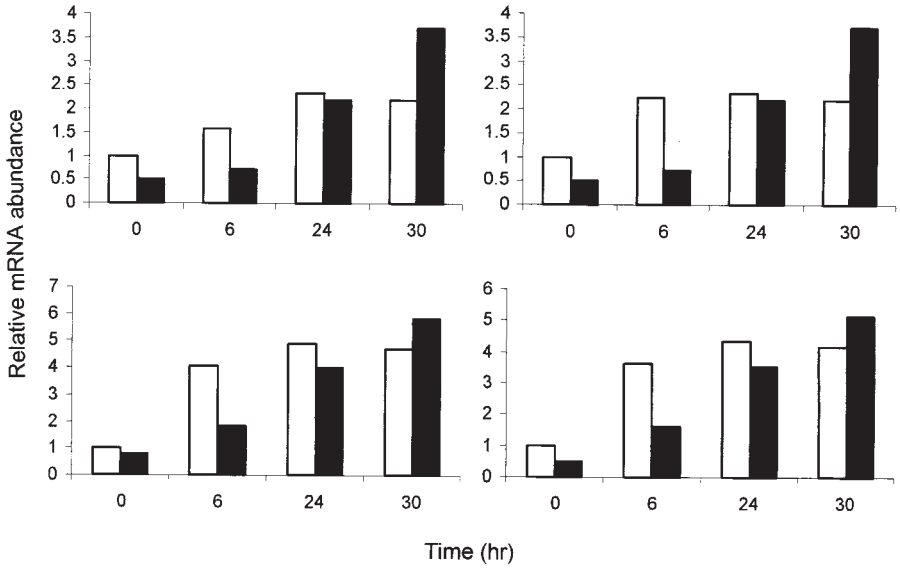

Figure 8. Induction of Fe–SOD Transcripts in Wild-Type Tobacco and cpGSHI-24.

Six-week-old plants were maintained in darkness for 72 hr before reexposure to the light under controlled-environment conditions. Samples were collected for RNA isolation at 0, 6, 24, and 30 hr. Slot blots (15 μg RNA per slot) were probed with an Fe–SOD fragment from *N. plumbaginifolia*, and hybridization signals were quantified by using a PhosphorImager. Equal RNA loading was confirmed by probing for rRNA. Data are shown for four independent experiments and are expressed relative to wild-type transcript levels at the start of the light period. Open bars are wild type, and solid bars are cpGSHI-24.

nonstress conditions in the light do not accumulate foliar γ-EC to high levels compared with GSH and cysteine (Table 1 and Figure 5; Noctor et al., 1996, 1997; Polle, 1996). To our knowledge, there are no reports that wild-type plants have detectable levels of ESSE, and we are not aware of any enzyme in plants that could reduce this compound back to γ-EC. Therefore, γ-EC may not participate in any redox cycle in the plant, and because it is a biosynthetic intermediate on the pathway to GSH (Figure 1A), the flux through this small pool must ensure that its oxidized form does not accumulate to any significant degree. Therefore, the only route open to removal of ESSE is possibly by degradation in a way described for γ-EC (Noctor et al., 1998).

The cpGSHI/II hybrids had greatly increased GSH levels compared with their cpGSHI siblings (Figure 5). This presumably reflects the fact that both transgene-encoded enzymes were at high enough concentrations to escape limitations of feedback regulation or that the *E. coli*–derived enzymes are not subject to the same type of control as the native tobacco plastid enzymes. This point, plus the higher redox state of the γ-EC pool in the cpGSHI/II hybrids compared with the cpGSHI plants, strongly suggests that the γ-EC pool in the cpGSHI/II hybrids is turned over more rapidly (as a consequence of increased GS activity), which may slow the rate at which this pool is oxidized.

Photosynthetic Performance of cpGSHI Dysfunctional Chloroplasts

The severity of the chlorotic/necrotic symptoms depended on the prevailing light intensity (growth PPFD; Figure 3) and was associated with a degeneration of chloroplasts as the symptoms developed (Figure 7). Chloroplasts from young, non-symptomatic leaves in the cpGSHI lines, and to a lesser extent in the cpGSHI/II hybrids, were less efficient at photosynthetic carbon fixation at growth PPFD, and this inefficiency increased as leaf discs were exposed to higher light intensities (Figure 6). Furthermore, chloroplasts from the young green leaves of such plants showed the accumulation of spherical bodies sandwiched between the stroma thylakoids, which disappeared as the chloroplasts degenerated (Figure 7). Although the nature of these spherical bodies is not known, they indicate that the chloroplasts of nonchlorotic leaves were different from those of wild-type plants even at this pre-symptomatic stage.

Decreased abilities for photosynthetic carbon fixation in the cpGSHI lines, and to a lesser extent in the cpGSHI/II hybrids, could have enhanced photosynthetic reduction of O_2 (the Mehler reaction; see Introduction). This would in turn cause more ROS production and further oxidation of the GSH pool, the combination of which would lead to still

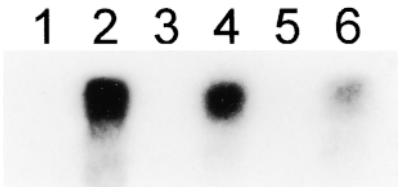

Figure 9. PR-1a Transcript Is Induced in Necrotic Tissue from the Leaves of T_3 Progeny of cpGSHI Lines.

RNA gel blot of 15 μg of total RNA from leaves of each of the lines cpGSHI-8, cpGSHI-24, and cpGSHI-26 (lanes 2, 4, and 6, respectively) or their recessive siblings (lanes 1, 3, and 5), respectively. RNA was subjected to electrophoresis through a denaturing agarose gel, blotted onto a nylon membrane, and probed with a ^{32}P-labeled PR-1a DNA fragment generated by polymerase chain reaction (PCR) amplification of tobacco genomic DNA. The blot was washed at high stringency, and the bands were visualized by autoradiography.

greater inhibition of carbon fixation. Thus, a downward spiral of oxidative destruction would be set in train, leading to premature senescence of the chloroplast and eventual death of the cell. Clearly, the higher the prevailing light conditions, the faster this destructive process would ensue—a situation that was readily observed in our experiments.

The Initiation of Oxidative Destruction of the Chloroplast: A Failure in Redox Sensing?

A striking feature of the cpGSHI transgenic plants grown under the standard controlled-environment conditions was that despite the clear oxidative stress, none of the transcripts encoding components of the antioxidant system in tobacco was elevated. These transcripts include those encoding catalase and SOD and APX isoforms as well as those encoding PH–GPX and GR isoforms. In various environmental conditions known to promote oxidative stress in tobacco or related *Nicotiana* spp, the levels of at least some of these transcripts have been shown to be increased (Bowler et al., 1989; Tsang et al., 1991; Criqui et al., 1992; Willekens et al., 1995; Mittler et al., 1996). Furthermore, the induction of Fe–SOD transcripts under conditions of oxidative stress, induced by transferring dark-adapted leaves to the light, was delayed in the cpGSHI lines compared with the wild type, but the Fe–SOD transcripts continued to accumulate in the cpGSHI lines to higher levels than did those in the wild-type control (Figure 8). It has previously been established that increases in Fe–SOD mRNA in such a transition is a consequence of increased internally generated oxidative stress in the chloroplast brought about by the onset of photosynthesis (Tsang et al., 1991). Thus, the altered pattern of accumulation of Fe–SOD mRNA in these plants undergoing a dark–light transition indicates that they may be disrupted in redox sensing. Such a mechanism would normally monitor ROS production throughout the life of the leaf and adjust the activity of the antioxidant system as appropriate.

These plants also display increased sensitivity to abiotic stresses such as ozone fumigation (Wellburn et al., 1998) and chilling (M. Fryer, G. Creissen, P. Mullineaux, and N. Baker, manuscript in preparation), which is consistent with this hypothesis. That GSH may play a role in redox sensing as well as the response to oxidative stress is supported by the observation that pretreatment of Arabidopsis leaves with GSH before the application of a photoinhibitory light stress renders photosynthesis more sensitive to the stress than control treatments and is associated with a marked failure to increase the levels of APX transcripts normally induced under this stress in this species (Karpinski et al., 1997).

From these experiments, it was proposed that changes in the redox state of the foliar GSH pool may be a factor in sensing oxidative stress. It has been suggested (Foyer et al., 1997) that the balance between ROS synthesis and destruction allows for some controlled oxidation, which may be important in signaling detrimental changes in the environment, thus permitting redirection of resources to minimize damage. Disruption of this balance in either direction may have similar consequences for the plant.

Comparison of cpGSHI Plants with Catalase-Suppressed Transgenic Plants

Transgenic tobacco plants with lowered levels of peroxisomal catalase activity show a light intensity–dependent necrotic phenotype that can be completely ameliorated by growing such plants under nonphotorespiratory conditions. Furthermore, these plants have higher foliar GSH levels that are in a more oxidized state than their wild-type counter-

Table 3. Catalase Activities in Cell-Free Leaf Extracts[a]

Parental Line	Genotype	Catalase Activity[b]
cpGSHI-8	cpGSHI	666.8 ± 12.8
cpGSHI-8	Wild type	205.6 ± 6.2
cpGSHI-24	cpGSHI-8	542.5 ± 10.8
cpGSHI-24	Wild type	190 ± 13.3

[a] Extracts were made from leaves of 4-week-old, controlled-environment-grown cpGSHI-8, cpGSHI-24, and transgene-recessive siblings.

[b] Catalase activity was determined according to the method of Aebi (1984) and is expressed as micromoles of H_2O_2 reduced per gram fresh weight per miniute.

parts, and in severely necrotic tissues the level of the PR-1a transcript is markedly induced (Chamnongpol et al., 1996; Willekens et al., 1997). These properties are clearly analogous to those described for the cpGSHI lines (Figures 3 to 5 and 9, and Table 1). However, there are also fundamental differences in the two sets of transgenic plants that make it unlikely that a failure in peroxisome function is the cause of the oxidative stress phenotype displayed by the cpGSHI transgenic lines. These differences are as follows: (1) prenecrotic leaves of catalase-suppressed plants appear to photosynthesize normally in contrast to green sectors of cpGSHI lines (Figure 6; Willekens et al., 1997); (2) the chlorotic phenotype in the cpGSHI transgenic lines is associated with an increase in foliar H_2O_2 levels in contrast to the catalase-suppressed plants; and (3) there was no inhibition of catalase activity or reduction in the level of catalase transcripts in the cpGSHI-containing lines (Table 3).

The properties of the catalase-suppressed plants have led to the hypothesis that the peroxisome is a major sink for H_2O_2 in the leaves of C_3 plants, irrespective of its source (Willekens et al., 1997). If this is the case, then in the cpGSHI plants this sink failed to deal with the H_2O_2 under photorespiratory (i.e., ambient CO_2 concentrations) conditions.

Comparison of cpGSHI Plants with Lesion Mimic Mutants

The observed symptoms of the cpGSHI transgenic lines superficially show parallels to lesion mimic mutants, in particular the *lsd* (for lesion simulating disease) and *acd* (for accelerated cell death) mutants of Arabidopsis (Deitrich et al., 1994; Greenberg et al., 1994; Jabs et al., 1996). The *lsd* mutants grown under extended photoperiods and the transgenic tobacco grown under controlled-environment conditions show a similar spreading chlorotic phenotype, and both are clearly perturbed in ROS metabolism (Deitrich et al., 1994; Jabs et al., 1996). However, in the cpGSHI lines, none of the transcripts normally associated with responses to pathogens (e.g., those encoding PR-1a, CHS, and PAL) has higher levels in these chlorotic tissues (see Results). Only under conditions of severe necrosis in greenhouse-grown material did we observe an increase in PR-1a transcript levels (Figure 9). Although in the cpGSHI lines we have not investigated other possible properties of lesion mimic mutants, we consider the failure to observe any increase in pathogenesis-associated mRNAs in chlorotic tissue as an indication that this comparison is at best limited. Whereas a role for oxidative stress in the chloroplast has been ruled out as initiating the phenotype of the *lsd* mutants in Arabidopsis (Jabs et al., 1996), the recent demonstration that H_2O_2 levels in tobacco chloroplasts transiently increase during initial contact with a pathogen (Allen and Fluhr, 1997) suggests that the role of the chloroplast in the early stages of the hypersensitive response might be more prominent than hitherto acknowledged.

METHODS

Polymerase Chain Reaction Amplification and Cloning of *gshI* and *gshII* Coding Sequences from *Escherichia coli* B DNA

Cloning of the genes encoding γ-glutamylcysteine synthetase (γ-ECS) and glutathione synthetase (GS), *gshI* and *gshII,* respectively, was achieved from polymerase chain reaction (PCR)–amplified DNA by using the following specific primers. For *gshI*, the primers were 5′-CATGATGTGGTGGCACTAATTGTAG-3′ (nucleotide positions 247 to 271; Watanabe et al., 1986) and 5′-CTGTCAGGCGTGTTTTTC-CAGCCAC-3′ (nucleotide positions 1897 to 1873). For *gshII*, the primers were 5′-TGATTGGCCCGGAAGGCGGTTTATC-3′ (nucleotide positions 196 to 220; Gushima et al., 1984) and 5′-TCA-GAGTCTCAACGAGATCCTTCTC-3′ (nucleotide positions 1352 to 1328). The PCR conditions were 40 cycles of 30 sec at 92°C, 30 sec at 55°C, and 90 sec at 72°C, using 1 ng of *E. coli* B DNA (Sigma) and 15 pmol of each primer in a 100-μL reaction. At the end of the cycles, the reactions were incubated at 72°C for 20 min. PCR fragments of the predicted lengths (1.65 kb for *gshI* and 1.15 kb for *gshII*) were eluted from a 1% (w/v) agarose gel and ligated into the dideoxy T-tailed EcoRV site of pBluescript II KS+ (Stratagene, La Jolla, CA; Alting-Mees and Short, 1989) by using standard in vitro recombination techniques (Sambrook et al., 1989). The plasmid-borne cloned *gshI* and *gshII* genes were confirmed to be functional by their ability to complement the corresponding *gshI*- or *gshII*-defective *E. coli* mutants (Apontoweil and Berends, 1975), permitting their growth on minimal medium containing 100 μg mL^{-1} tetramethylthiuramdisulfide (TMTD). TMTD is detoxified in bacteria by its conjugation with glutathione (GSH; Apontoweil and Berends, 1975). To facilitate further manipulations, an SphI site (GCATGC) was introduced by site-directed mutagenesis such that the underlined sequence provided the translation initiation codon of both genes (Gushima et al., 1984; Watanabe et al., 1986). The mutants were verified by sequencing, and a repeat of the complementation tests was performed, as described above. The plasmids harboring the SphI-containing *gshI* and *gshII* genes were designated pGSH1-S and pGSH2-S, respectively.

Gene Constructs, Plant Material, and Transformation

Two binary vectors were constructed. The coding sequence of *gshI* of pGSH1-S was fused to the rbcS sequence encoding the chloroplast transit peptide from the small subunit of ribulose-1,5-bisphosphate carboxylase/oxygenase from pea and placed under the control of the cauliflower mosaic virus (CaMV) 35S promoter with duplicated enhancer region and CaMV polyadenylation sequences (pJIT117; Guerineau et al., 1988) to create chloroplast GSHI (cpGSHI). The transit peptide and GSHI coding sequences were fused via their respective SphI sites. This chimeric gene construct was ligated into the polylinker of pBIN19 (Bevan, 1984) to produce pGSH106 (Figure 1B). A similar construct (pGSH209) containing the *gshII* coding sequence fused to the rbcS transit peptide sequence (cpGSHII) and placed in pBIN19 was made (Figure 1B). Both constructs were mobilized into *Agrobacterium tumefaciens* LBA4404 by the triparental mating procedure (Ditta et al., 1980).

Plants (*Nicotiana tabacum* cv Samsun NN) were maintained in a greenhouse with supplementary lighting to provide an 18-hr day length. Production of transgenic tobacco was achieved by leaf disc cocultivation, as described elsewhere (Creissen et al., 1995).

Transgenic plants were grown either in the greenhouse or in a controlled-environment room (16-hr day at 25°C and at 80% relative humidity, with a 250 μmol m^{-2} sec^{-1} photosynthetically active photon flux density [PPFD]).

RNA Extraction and Analysis

RNA was purified from deproteinized leaf extracts by lithium chloride precipitation, as described elsewhere (Creissen and Mullineaux, 1995). For RNA gel blot analysis, total RNA (15 μg) was resolved on 1% (w/v) agarose denaturing (formaldehyde) gels. RNA was transferred to nylon membranes (Hybond N; Amersham, Little Chalfont, UK) by capillary blotting, and hybridizations were performed using standard procedures (Sambrook et al., 1989). Filters were washed at high stringency (0.1 × SSC [1 × SSC is 0.15 M NaCl and 0.015 M sodium citrate] and 0.1% SDS at 65°C) for homologous probes and at reduced stringency (2 × SSC and 0.1% SDS at 65°C) for heterologous probes before visualization by autoradiography or by use of a PhosphorImager (Fuji Photofilm, Kanagawa, Japan).

GSH, γ-Glutamylcysteine, and H_2O_2 Determinations

Thiols were determined as their monobromobimane (MB)-derivatized products (Newton et al., 1981). Leaf discs for determination of GSH and γ-glutamylcysteine (γ-EC) were cut from 6-week-old plants (nodes 4 to 6 counted from the top of the plant), immediately frozen in liquid nitrogen, and stored at −80°C until analysis was performed. Leaf material (50 mg) was extracted with 1 mL of 0.1 M HCl and centrifuged in a microcentrifuge (5 min at 4°C). Cleared supernatants were neutralized by adding an equal volume of 0.1 M NaOH, and aliquots (50 μL) were derivatized by adding to 1.5-mL tubes containing 35 μL of water, 10 μL of Tris-HCl, pH 8.0, and 5 μL of 10 mM MB (Calbiochem). Samples were incubated at room temperature for 15 min before the addition of 900 μL 5% acetic acid. For determining total (reduced and oxidized) thiols, extracts were first reduced by the addition of DTT (2.5 mM final concentration), and subsequently the MB final concentration used was 5 mM.

Separation of MB-derivatized thiols was achieved by C18 reversed-phase HPLC, and their detection using an on-line fluorometer was according to the method of Newton et al. (1981). Identification and quantification of thiol compounds were performed by comparison of retention times of known amounts of standard compounds derivatized with MB. GSH was obtained from Boehringer Mannheim, and γ-EC was a kind gift from C. Foyer (IGER, Aberystwyth, UK). Di-γ-glutamylcystine (ESSE) was prepared by incubation of a 15-mM solution of γ-EC with 200 mM H_2O_2 for 48 hr at 37°C, at the end of which time there was no detectable thiol by reaction with 5,5′-dithiobis(2-nitrobenzoic acid) (Smith et al., 1989). The ESSE was freeze-dried and used to prepare standard solutions.

We also used amperometric detection of GSH and GSSG after separation on a Dionex (Sunnyvale, CA) HPLC, primarily to determine the redox state of the GSH pool in cpGSHI × GR46 hybrid samples (see Results and Table 2). The method is derived from application note 110 from Dionex and is as follows. Leaf samples (0.05 g) were harvested and plunged into liquid nitrogen and then ground in 1.5% (v/v) acetonitrile/0.1 N perchloric acid, left on ice for 30 min, and centrifuged in a chilled microcentrifuge at top speed for 10 min. The supernatant was filtered through a 0.2-μm Anotop 10/1C inorganic membrane filter (Whatman). Filtered supernatant (0.1 mL) was recovered, and 0.05 mL was injected onto the HPLC column. Separation of GSH and GSSG was achieved by reversed-phase HPLC by using a Dionex DX500 BioLC machine fitted with a Zorbax (Dionex, Camberley, UK) RP300-C18 column (150 × 4.6 mm) and a mobile phase of 1.5% (v/v) acetonitrile in 0.1 N perchloric acid at a flow rate of 0.8 mL/min. Integrated amperometric detection was used with a gold working electrode and sodium reference electrode. Integrated peak areas were compared with those from 30 to 300 pmol GSH and GSSG standards to calculate amounts of these compounds in leaf extracts. This method could not be used to separate γ-EC from cysteine and thus was not applied for these purposes.

H_2O_2 was determined by a modified fluorescence procedure (Guilbault et al., 1967). Leaf discs (19-mm diameter) were cut and immediately frozen in liquid nitrogen. The tissue was extracted in 500 μL of 25 mM HCl in a mortar and centrifuged at 5000*g* for 5 min at 4°C. Pigments were removed by vortexing in the presence of activated charcoal and centrifuging to remove most of the charcoal, and then 200 μL of the supernatant was centrifuged through a Wizard mini-column (Promega, Madison, WI) to remove any remaining particulate matter. For the assay, 50 μL of the cleared extract was mixed in a 3-mL fluorescence cuvette with 2.89 mL of 50 mM Hepes, pH 7.5, and 30 μL of 50 mM homovanillic acid in 50 mM Hepes, pH 7.5. The reaction was started by the addition of 30 μL of 4 μM horseradish peroxidase. The H_2O_2 concentration was obtained by measuring relative fluorescence (excitation of 315 nm; emission of 425 nm) against a standard curve.

Measurement of the Activities of γ-ECS, GSH Reductase, and Catalase

Measurements of extractable γ-ECS activity were conducted in an anaerobic chamber on samples collected from controlled-environment-grown plants and frozen in liquid nitrogen. Preweighed leaf discs were ground in a mortar in 0.1 M Tris-HCl, pH 7.5, 5 mM EDTA (10 mL g^{-1}) with 1 g g^{-1} polyvinylpolypyrrolidone and acid-washed sand. Cleared supernatant was obtained by centrifuging twice for 15 min at 15,000*g*. The γ-ECS assay was performed in a 500-μL reaction containing 0.1 M Tris-HCl, pH 7.5, 0.1 M $MgCl_2$, 10 mM ATP, 50 mM Na-L-glutamate, 8 mM phosphocreatine, 2 units of creatine phosphokinase, and 200 μL of cleared supernatant. The mixture was incubated under anaerobic conditions at 37°C for 10 min before the reaction was started by adding 50 μL of 20 mM L-cysteine. L-cysteine was dissolved in N_2-sparged water just before use. Samples (50 μL) were collected at 10-min intervals, the reaction was stopped, and the products were derivatized with MB and separated and quantified by HPLC, as described above. γ-ECS activity was quantified as nanomoles of γ-EC formed per minute per gram fresh weight leaf material.

GSH reductase activity was measured as described by Creissen et al. (1995), and catalase activity was determined by the method of Aebi (1984).

Chloroplast Isolation

Chloroplasts were isolated as previously described (Creissen et al., 1995). The absence of cytosol contamination of chloroplast fractions was confirmed by assaying for the cytosol-specific markers pyrophosphate-dependent phosphofructokinase (Journet and Douce,

1985) and glucose-6-phosphate dehydrogenase (Doehlert et al., 1988). Chloroplast fractions that were free of detectable cytosol marker enzyme activity were used for immunodetection of the transgene-encoded proteins, as described below.

Immunodetection of cpGSHI and cpGSHII in Foliar Extracts

Cell-free protein extracts were prepared as described above but without using an anaerobic chamber. Total protein (10 to 30 μg) was subjected to SDS-PAGE and electroblotted to nitrocellulose; the use of polyclonal antibodies to immunodetect specific polypeptides has been described previously (Stevens et al., 1997). Polyclonal antibodies raised against the purified *E. coli*–derived γ-ECS and GS polypeptides were used at 1:1000 dilution to detect the corresponding proteins in the plant extracts and did not cross-react against any plant-derived polypeptide (Arisi et al., 1997). The antisera were kind gifts from A.-C.M. Arisi (INRA, Versailles, France) and C.H. Foyer (IGER, Aberystwyth, UK).

Photosynthetic Gas Exchange Measurements

Net photosynthetic CO_2 uptake was measured on third leaves, essentially as described previously by Bongi and Long (1987), in an assimilation chamber on a small area of the leaf surface (2.0 cm^2), illuminated by a quartz-iodide source. The light incident on the leaf was varied by interposing neutral density filters. The PPFD at the leaf surface was determined by placing a quantum sensor below the chamber window in the position normally occupied by the leaf (LI-190 SR; Li-Cor, Lincoln, NE). Measurements were started after net CO_2 uptake reached a steady state in air containing 360 ± 10 μmol mol^{-1} CO_2 at a temperature of 24°C. Leaf gas exchange parameters were calculated according to the equations of Von Caemmerer and Farquar (1981), and light dose–response curves were constructed for intensities between 100 and 1200 μmol m^{-2} sec^{-1} incident PPFD.

Ultrastructural Studies

Leaf tissue fixation and preparation for electron microscopy were performed as previously described (Wellburn and Wellburn, 1994).

ACKNOWLEDGMENTS

We are grateful to Drs. Ana Arisi and Christine Foyer for the gifts of γ-ECS and GS antisera and to the latter for the gift of purified γ-EC. We thank Drs. Rod Casey, Carolina Escobar, and Ana Jiménez for critical reading of the manuscript. This work was supported by the Biotechnology and Biological Sciences Research Council (BBSRC) Global Environmental Change Initiative, the Commission of the European Communities (CEC) Agro-Industrial Research (AIR) Programme (Contract No. AIR1-CT92-0205), and the BBSRC Core Strategic Grant to the John Innes Centre. G.P. is supported by a CEC AIR Fellowship.

Received January 11, 1999; accepted April 6, 1999.

REFERENCES

Aebi, H. (1984). Catalase *in vitro*. Methods Enzymol. **105,** 121–126.

Allen, A.C., and Fluhr, R. (1997). Two distinct sources of elicited reactive oxygen species in tobacco epidermal cells. Plant Cell **9,** 1559–1572.

Alting-Mees, M.A., and Short, J.M. (1989). pBluescript II, gene mapping vectors. Nucleic Acids Res. **17,** 9494.

Anderson, S., and Smith, S.M. (1986). Synthesis of the small subunit of ribulose-bisphosphate carboxylase from genes cloned into plasmids containing the SP6 promoter. Biochem. J. **240,** 709–715.

Apontoweil, P., and Berends, W. (1975). Isolation and initial characterization of glutathione-deficient mutants of *Escherichia coli* K12. Biochim. Biophys. Acta **399,** 10–22.

Arisi, A.-C.M., Noctor, G., Foyer, C.H., and Jouanin, L. (1997). Modification of thiol contents in poplars (*Populus tremula* × *P. alba*) overexpressing enzymes involved in glutathione synthesis. Planta **203,** 362–372.

Asada, K. (1994). Production and action of active oxygen species in photosynthetic tissues. In Causes of Photooxidative Stress and Amelioration of Defense Systems in Plants, C.H. Foyer and P.M. Mullineaux, eds (Boca Raton, FL: CRC Press), pp. 77–104.

Baker, C.J., and Orlandi, E.W. (1995). Active oxygen in plant pathogenesis. Annu. Rev. Phytopathol. **33,** 299–321.

Baker, N.R. (1994). Chilling stress and photosynthesis. In Causes of Photooxidative Stress and Amelioration of Defense Systems in Plants, C.H. Foyer and P.M. Mullineaux, eds (Boca Raton, FL: CRC Press), pp. 127–154.

Bevan, M. (1984). Binary *Agrobacterium* vectors for plant transformation. Nucleic Acids Res. **12,** 8711–8721.

Bielawski, W., and Joy, K.W. (1986). Reduced and oxidised glutathione and glutathione-reductase activity in tissues of *Pisum sativum*. Planta **169,** 267–272.

Bongi, G., and Long, S.P. (1987). Light dependent damage to photosynthesis in olive leaves during chilling and high-temperature stress. Plant Cell Environ. **10,** 241–249.

Bowler, C., Alliotte, T., De Loose, M., Van Montagu, M., and Inzé, D. (1989). The induction of manganese superoxide dismutase in response to stress in *Nicotiana plumbaginifolia*. EMBO J. **8,** 31–38.

Broadbent, P., Creissen, G.P., Kular, B., Wellburn, A.R., and Mullineaux, P.M. (1995). Oxidative stress responses in transgenic tobacco containing altered levels of glutathione reductase activity. Plant J. **8,** 247–255.

Chamnongpol, S., Willekens, H., Langebartels, C., Van Montagu, M., Inzé, D., and Van Camp, W. (1996). Transgenic tobacco with a reduced catalase activity develops necrotic lesions and induces pathogenesis-related expression under high light. Plant J. **10,** 491–503.

Conklin, P.L., and Last, R.L. (1995). Differential accumulation of antioxidant mRNAs in *Arabidopsis thaliana* exposed to ozone. Plant Physiol. **109,** 203–212.

Creissen, G.P., and Mullineaux, P.M. (1995). Cloning and characterisation of glutathione reductase cDNAs and identification of two genes encoding the tobacco enzyme. Planta **197,** 422–425.

Creissen, G., Reynolds, H., Xue, Y., and Mullineaux, P. (1995). Simultaneous targeting of pea glutathione reductase and of a bacterial fusion protein to chloroplasts and mitochondria in transgenic tobacco. Plant J. **8,** 167–175.

Criqui, M.C., Jamet, E., Parmentier, Y., Marbach, J., Durr, A., and Flack, J. (1992). Isolation and characterization of a plant cDNA showing homology to animal glutathione peroxidases. Plant Mol. Biol. **18,** 623–627.

Deitrich, R.A., Delaney, T.P., Uknes, S.J., Ward, E.R., Ryals, J.A., and Dangl, J.L. (1994). *Arabidopsis* mutants simulating disease resistance response. Cell **77,** 565–577.

Ditta, G., Stanfield, S., Corbin, D., and Helinski, D.R. (1980). Broad host range DNA cloning system for Gram-negative bacteria: Construction of a gene bank of *Rhizobium meliloti*. Proc. Natl. Acad. Sci. USA **77,** 7347–7351.

Doehlert, D.C., Kuo, T.M., and Felker, F.C. (1988). Enzymes of sucrose and hexose metabolism in developing kernels of two inbreds of maize. Plant Physiol. **86,** 1013–1019.

Foyer, C.H., and Halliwell, B. (1976). The presence of glutathione and glutathione reductase in chloroplasts: A proposed role in ascorbate metabolism. Planta **133,** 21–25.

Foyer, C.H., and Harbinson, J. (1994). Oxygen metabolism and the regulation of photosynthetic electron transport. In Causes of Photooxidative Stress and Amelioration of Defense Systems in Plants, C.H. Foyer and P.M. Mullineaux, eds (Boca Raton, FL: CRC Press), pp. 1–42.

Foyer, C.H., Lopez-Delgado, H., Dat, J.F., and Scott, I.M. (1997). Hydrogen peroxide– and glutathione-associated mechanisms of acclimatory stress tolerance and signaling. Physiol. Plant. **100,** 241–254.

Fryer, M. (1993). The antioxidant effects of thylakoid vitamin E (α-tocopherol). Plant Cell Environ. **15,** 381–392.

Grantz, A.A., Brummell, D.A., and Bennett, A.B. (1995). Ascorbate free radical reductase mRNA levels are induced by wounding. Plant Physiol. **108,** 411–418.

Greenberg, J.T., Guo, A., Klessig, D.F., and Ausubel, F.M. (1994). Programmed cell death in plants: A pathogen-triggered response activated coordinately with multiple defense functions. Cell **77,** 551–563.

Guerineau, F., Woolston, S., Brooks, L., and Mullineaux, P. (1988). An expression cassette for targeting foreign proteins into chloroplasts. Nucleic Acids Res. **16,** 11380.

Guilbault, G.G., Kramer, D.N., and Hackley, E. (1967). A new substrate for fluorometric determination of oxidative enzymes. Anal. Chem. **39,** 271.

Gushima, H., Yasuda, S., Soeda, E., Yokota, M., Kondo, M., and Kimura, A. (1984). Complete nucleotide sequence of the *E. coli* glutathione synthetase gsh-II. Nucleic Acids Res. **12,** 9299–9307.

Hell, R., and Bergmann, L. (1990). γ-Glutamylcysteine synthetase in higher plants: Catalytic properties and subcellular localization. Planta **180,** 603–612.

Hérouart, D., Van Montagu, M., and Inzé, D. (1993). Redox-activated expression of the cytosolic copper/zinc superoxide dismutase gene in *Nicotiana*. Proc. Natl. Acad. Sci. USA **90,** 3108–3112.

Jabs, T., Dietrich, R.A., and Dangl, J.L. (1996). Initiation of runaway cell death in an *Arabidopsis* mutant by extracellular superoxide. Science **273,** 1853–1856.

Journet, E.-P., and Douce, R. (1985). Enzymatic capacities of purified cauliflower bud plastids for lipid synthesis and carbohydrate metabolism. Plant Physiol. **79,** 458–467.

Karpinski, S., Escobar, C., Karpinska, B., Creissen, G., and Mullineaux, P.M. (1997). Photosynthetic electron transport regulates the expression of cytosolic ascorbate peroxidase genes in Arabidopsis during excess light stress. Plant Cell **9,** 627–640.

Law, M.Y., Charles, S.A., and Halliwell, B. (1983). Glutathione and ascorbic acid in spinach (*Spinacia oleracea*) chloroplasts. Biochem J. **210,** 899–903.

Levine, A., Tenhaken, R., Dixon, R., and Lamb, C.J. (1994). H_2O_2 from the oxidative burst orchestrates the plant hypersensitive disease resistance response. Cell **79,** 583–593.

Link, G. (1996). Green life: Control of chloroplast gene transcription. Bioessays **18,** 465–471.

May, M., Hammond-Kosack, K.E., and Jones, J.D.G. (1996). Involvement of reactive oxygen species, glutathione metabolism, and lipid peroxidation in the *Cf*-gene-dependent defense response of tomato cotyledons induced by race-specific elicitors of *Cladosporium fulvum*. Plant Physiol. **110,** 1367–1379.

Meyer, M., Schreck, R., and Baeuerle, P.A. (1993). H_2O_2 and antioxidants have opposite effects on activation of NF-κB and AP-1 in intact cells: AP-1 as secondary antioxidant-responsive factor. EMBO J. **12,** 2005–2015.

Mittler, R., Shulaev, V., Seskar, M., and Lam, E. (1996). Inhibition of programmed cell death in tobacco plants during a pathogen-induced hypersensitive response at low oxygen pressure. Plant Cell **8,** 1991–2001.

Mullineaux, P., and Creissen, G. (1996). Opportunities for the genetic manipulation of antioxidants in plant foods. Biochem. Soc. Trans. **24,** 829–835.

Mullineaux, P.M., and Creissen, G.P. (1997). Glutathione reductase: Regulation and role in oxidative stress. In Oxidative Stress and the Molecular Biology of Antioxidant Defenses, J. Scandalios, ed (Cold Spring Harbor, NY: Cold Spring Harbor Laboratory Press), pp. 667–713.

Mullineaux, P.M., Karpinski, S., Jiménez, A., Cleary, S.P., Robinson, C., and Creissen, G.P. (1998). Identification of cDNAs encoding plastid-targeted glutathione peroxidase. Plant J. **13,** 375–379.

Newton, G.L., Dorian, R., and Fahey, R.C. (1981). Analysis of biological thiols: Derivitization with monobromobimane and separation by reverse-phase high performance liquid chromatography. Anal. Biochem. **114,** 383–387.

Noctor, G., Strohm, M., Jouanin, L., Kunert, K.-J., Foyer, C.H., and Rennenberg, H. (1996). Synthesis of glutathione in leaves of transgenic poplar overexpressing γ-glutamylcysteine synthetase. Plant Physiol. **112,** 1071–1078.

Noctor, G., Arisi, A.-C.M., Jouanin, L., Valadier, M.-H., Roux, Y., and Foyer, C.H. (1997). The role of glycine in determining the rate of glutathione synthesis in poplar: Possible implications for glutathione production during stress. Physiol. Plant. **100,** 255–263.

Noctor, G., Arisi, A.-C.M., Jouanin, L., Kunert, K.J., Rennenberg, H., and Foyer, C.H. (1998). Glutathione: Biosynthesis, metabolism and relationship to stress tolerance in transformed plants. J. Exp. Bot. **49,** 623–647.

Pennell, R.I., and Lamb, C. (1997). Programmed cell death in plants. Plant Cell **9,** 1157–1168.

Polle, A. (1996). Developmental changes of antioxidative systems in tobacco leaves as affected by limited sucrose export in transgenic plants expressing yeast-invertase in the apoplastic space. Planta **198,** 253–262.

Ruegsegger, A., and Brunold, C. (1993). Localization of γ-glutamylcysteine synthetase and glutathione synthetase activity in maize seedlings. Plant Physiol. **101,** 561–566.

Sambrook, J., Fritsch, E.F., and Maniatis, T. (1989). Molecular Cloning: A Laboratory Manual, 2nd ed. (Cold Spring Harbor, NY: Cold Spring Harbor Laboratory Press).

Smith, I.K., Vierhaller, T.L., and Thorne, C.A. (1989). Properties and functions of glutathione reductase in plants. Physiol. Plant. **77,** 449–456.

Stevens, R.G., Creissen, G.P., and Mullineaux, P.M. (1997). Cloning and characterisation of a cytosolic glutathione reductase cDNA from pea (*Pisum sativum* L.) and its expression in response to stress. Plant Mol. Biol. **35,** 641–654.

Strohm, M., Jouanin, L., Kunert, K.-J., Pruvost, C., Polle, A., Foyer, C.H., and Rennenberg, H. (1995). Regulation of glutathione synthesis in leaves of transgenic poplar (*Populus tremula* × *P. alba*) overexpressing glutathione synthetase. Plant J. **7,** 141–145.

Tsang, E.W.T., Bowler, C., Hérouart, D., Van Camp, W., Villarroel, R., Genetello, C., Van Montagu, M., and Inzé, D. (1991). Differential regulation of superoxide dismutases in plants exposed to environmental stress. Plant Cell **3,** 783–792.

Von Caemmerer, S., and Farquar, G.D. (1981). Some relationships between the biochemistry of photosynthesis and the gas exchange of leaves. Planta **156,** 199–206.

Watanabe, K., Yamano, Y., Murata, K., and Kimura, A. (1986). The nucleotide sequence of the gene for γ-glutamylcysteine synthetase of *Escherichia coli*. Nucleic Acids Res. **14,** 4393–4400.

Wellburn, F.A.M., and Wellburn, A.R. (1994). Atmospheric ozone affects carbohydrate allocation and winter hardiness of *Pinus halpensis* (Mill.). J. Exp. Bot. **45,** 607–614.

Wellburn, F.A.M, Creissen, G.P., Lake, J.A., Mullineaux, P.M., and Wellburn, A.R. (1998). Tolerance to atmospheric ozone in transgenic tobacco over-expressing glutathione synthetase in plastids. Physiol. Plant. **104,** 623–629.

Willekens, H., Van Camp, W., Van Montagu, M., Inzé, D., Langebartels, C., and Sandermann, H. (1995). Ozone, sulfur dioxide and ultraviolet B have similar effects on mRNA accumulation of antioxidant genes in *Nicotiana plumbaginifolia* L. Plant Physiol. **106,** 1007–1014.

Willekens, H., Chamnongpol, S., Davey, M., Schraudner, M., Langebartels, C., Van Montagu, M., Inzé, D., and Van Camp, W. (1997). Catalase is a sink for H_2O_2 and is indispensable for stress defence in C_3 plants. EMBO J. **16,** 4806–4816.

Wingate, V.P.M., Lawton, M.A., and Lamb, C.J. (1989). Glutathione causes a massive and selective induction of plant defense genes. Plant Physiol. **87,** 206–210.

Wingsle, G., and Karpinski, S. (1996). Differential redox regulation by glutathione of glutathione reductase and CuZn–superoxide dismutase gene expression in *Pinus sylvestris* L. needles. Planta **198,** 151–157.